

Observation of Stimulated Compton Scattering from Resonant Electrons in a Laser-Produced Plasma

R. P. Drake,⁽¹⁾ H. A. Baldis,⁽²⁾ R. L. Berger,⁽³⁾ W. L. Kruer,⁽¹⁾ E. A. Williams,⁽¹⁾ Kent Estabrook,⁽¹⁾
T. W. Johnston,⁽⁴⁾ and P. E. Young⁽¹⁾

⁽¹⁾*Lawrence Livermore National Laboratory, Livermore, California 94550*

⁽²⁾*National Research Council, Ottawa, Canada K1A 0R6*

⁽³⁾*KMS Fusion, Inc., Ann Arbor, Michigan 48106*

⁽⁴⁾*Institut National de la Recherche Scientifique-Energie, Varennes, Quebec, Canada J3X 1S2*

(Received 23 October 1989)

An experimental study of stimulated Compton scattering (SCS) from resonant electrons in a laser-produced plasma is reported. Up to 1.9 kJ of 350-nm laser light was used to irradiate 3- μm -thick CH targets in 1.3- to 3.3-ns pulses at intensities up to 1.3×10^{15} W/cm². SCS was detected by making time-resolved measurements of the emission near 420 nm. The measurements are compared to the results of theoretical modeling.

PACS numbers: 52.40.Nk, 42.20.Ji, 52.25.Qt, 52.35.Nx

When laser light produces and irradiates a plasma, the laser-light wave can drive scattered-light waves by a number of different mechanisms. One of them is stimulated Compton scattering (SCS) from electrons, referred to herein as SCS-E. SCS-E is a kinetic scattering process in which a scattered-light wave is amplified by stimulated scattering from resonant electrons in the plasma. SCS-E is of interest to plasma physics as a distinct mechanism by which an intense electromagnetic wave in a plasma can drive other waves. SCS-E is also of interest to laser fusion, because a high-gain, laser-fusion plasma will include large volumes in which stimulated Raman backscattering¹ (SRS) is Landau damped, but throughout which SCS-E can still occur. SCS-E could reduce the gain of such a target by reflecting energy from it. It is thus important to determine what constraints this process may impose on laser fusion. The present paper reports the first experimental study of SCS-E.

SCS-E is related to the more familiar, three-wave parametric instabilities.² In the basic process, the incident- and scattered-light waves interact to drive via the ponderomotive force an electrostatic beat wave with a phase velocity $v_{\text{ph}} = (\omega_0 - \omega_s) / |\mathbf{k}_0 - \mathbf{k}_s|$. Here ω_0 (ω_s) and \mathbf{k}_0 (\mathbf{k}_s) are the frequency and wave number of the incident- (scattered-) light wave. If $v_{\text{ph}} \gg v_{\text{th}}$ (the electron thermal velocity) and $\omega_0 - \omega_s \sim \omega_{pe}$ (the electron plasma frequency), then the beat wave is resonantly enhanced by the plasma; that is, it becomes an electron plasma wave. This limit is the well-known stimulated Raman instability. If in contrast $v_{\text{ph}} \sim v_{\text{th}}$, then the beat wave is not a normal mode of the plasma but is instead a heavily damped, forced oscillation. Since energy flows from the incident wave into the damped oscillation, the Manley-Rowe relations show that energy is also transferred to the scattered-light wave. The instability in this limit is called SCS-E.

About fifteen years ago there was a period of intense

theoretical work on SCS-E, both as one of the possible mechanisms of stimulated scattering³ and as an object of study in itself.⁴ This early work considered the scattering when v_{ph} was comparable to v_{th} . Some more recent work has considered the behavior as v_{ph} became larger.^{5,6} Other work has considered the production of nonthermal velocity distributions, leading to the evolution of SRS (or stimulated Brillouin scattering) into SCS as a saturation mechanism.⁷ In the present experiments, we have detected emissions much stronger than thermal, emissions which increase very quickly with laser intensity, but in a frequency region far closer to the incident laser frequency than the SRS emissions previously reported.⁸ This allows us to identify the beat-wave phase velocities as being comparable to the electron thermal velocity and hence to identify the emissions as SCS-E.

The linearized, Vlasov theory of SCS-E finds the growth rate to be⁴

$$\gamma_0 = (k^2 v_0^2 / 8 \omega_s) \text{Im} \{ \chi_e (1 + \chi_i) / (1 + \chi_e + \chi_i) \}, \quad (1)$$

where χ_e (χ_i) is the usual electron (ion) susceptibility evaluated at the wave number, k , and frequency, ω , of the beat wave; and v_0 is the oscillating velocity of the electron in the laser-light wave. In the limit $k \lambda_D \gg 1$, where λ_D is the electron Debye length, the growth rate maximizes when $v_{\text{ph}} = v_{\text{th}}$, and is given by

$$\gamma_0 = 0.2 (\omega_{pe}^2 / \omega_s) (v_0 / v_{\text{th}})^2. \quad (2)$$

This limit corresponds to a somewhat hotter or lower-density plasma with a smaller growth rate than that discussed here, for which it was necessary to numerically evaluate Eq. (1) to determine γ_0 .

The present experiments used the Nova laser.⁹ The experimental technique, described previously,¹⁰ was devised to allow comparison of scattered-light emissions under similar hydrodynamic conditions but at different values of I_L , which is the average of the laser intensity

over the irradiation area. The present experiments irradiated 3- μm -thick CH targets with constant-intensity (to $\pm 20\%$) laser pulses of 1.3 to 3.3 ns in duration (measured to ± 100 ps), laser energies of 0.6 to 1.9 kJ (known to $\pm 15\%$), and I_L of 2.7×10^{13} to 1.3×10^{15} W/cm^2 (known to $\pm 30\%$). The targets exploded to produce a transparent, planar plasma with a slowly decreasing maximum density.

The measurement of SCS-E used a sensitive, discrete-channel spectrometer (DCS), described previously,¹¹ to measure the emission at 153° from \mathbf{k}_0 . It was sufficiently sensitive to make time-resolved measurements of the thermal emission from the plasma. One of its channels was centered at 418 nm, with a full width at half maximum of 21 nm. The scattered light measured by this channel had a frequency of $0.82\omega_0$ to $0.86\omega_0$. This is a larger relative frequency than that examined in previous studies of the quenching of SRS by the onset of Landau damping.^{10,12} The corresponding beat wave had a frequency of about $0.16\omega_0$ and a wave number of about $1.8k_0$, so that v_{ph} was about $0.09c$. This corresponds to 1.4 to 2.8 times v_{th} for electron temperatures of 2 to 0.5 keV, which span the inferred range of the present experiments. The relative variation in sensitivity of the measurement at 418 nm is a factor of 3, limited by flat-field variations in the sensitivity of the streak camera and by variations in the processing of the film used to record the streak-camera output.

Figure 1 shows the emission near 418 nm, measured

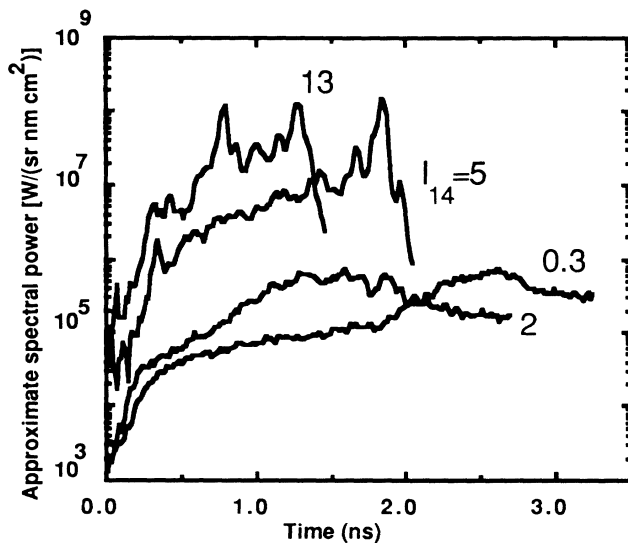


FIG. 1. The spectral power near 418 nm, which increases with laser intensity. The curves correspond to laser intensities, in units of 10^{14} W/cm^2 , of 0.3, 2.0, 4.7, and 13, to pulse durations of 3.3, 2.5, 1.8, and 1.3 ns, and to experiments 16091805, 16082210, 16102908, and 16100901, respectively. For the high-intensity experiments, the curves are truncated at the abrupt drop in emission at the end of the laser pulse, in order to show clearly the behavior during the laser pulse in all cases.

by the DCS, for experiments using four different values of I_L . Early in each experiment, the emission reaches a plateau value, rising from an instrumental-noise level that was determined by the filtering for that experiment. At the lowest I_L , the plateau value for the first 2 ns is approximately at thermal levels, based on previous observations and analysis.¹¹ Using the model described later and evaluations of T_e discussed previously,¹⁰ we calculate the thermal emission in this case to be 8×10^4 $\text{W}/(\text{sr nm cm}^2)$. Later in time, some enhancement above this level is observed.

For the other data in Fig. 1, the calculated thermal emission, in units of 10^5 $\text{W}/(\text{sr nm cm}^2)$, is 1.4, 1.9, and 2.6, corresponding to I_L of 2.0×10^{14} , 4.7×10^{14} , and 1.3×10^{15} W/cm^2 . The observed plateau level becomes much larger than this as I_L increases. For $I_L = 1.3 \times 10^{15}$ W/cm^2 , the plateau level is more than 2 orders of magnitude above the thermal emission. We attribute the difference to SCS-E. (We do not believe that the rapid modulations in the emission, observed above the plateau level at higher I_L , result from SCS-E, which is inherently nonlocal and should evolve slowly. Interpretation of these modulations is in progress.)

The level of the plateau in the emission also varies during the laser pulse. Changes in this level may reflect the temporal development of SCS-E. During most intervals in the data of Fig. 1, the emission increases slowly with time. This is sensible, because the gain region for SCS-E is in the very underdense plasma, and the scale length and volume of this region increase with time. In addition, T_e decreases as these targets expand.¹⁰ As a result v_{ph}/v_{th} increases and the amplitude of SCS-E may increase for this reason as well. The decrease of T_e also increases the collisional absorption of the light wave. At low I_L , this may explain the presence of a maximum in the emission before the end of the laser pulse. Simulations¹⁰ indicate these plasmas to be nearly isothermal, once the electron density has decreased to well below n_c , where n_c is the critical density of the 350-nm laser light.

To determine the spectral power, the measured emission (in $\text{W}/\text{sr nm}$) was assumed to originate from an area the size of the laser spot on the target. The absolute calibration of the DCS was estimated by comparison with data from a calibrated, continuous spectrometer, using the experiment producing the most intense emission in Fig. 1. The resulting calibration is plausible, as the emissions from low-intensity experiments are inferred to be near thermal levels. However, the ratio of signal to background in the continuous data is uncertain, as the signal is weak relative to the stronger emission at longer wavelengths. (Indeed, it is only observable because the S-1 photocathode is much more sensitive at 400 nm than at 500 nm.) As a result, the values of the spectral power shown here represent an upper limit to within the factor-of-3 uncertainty in the calibration of the continuous spectrometer.

The gain for SCS-E depends on an integral over the plasma profile.⁶ Thus, in order to compare the data of Fig. 1 to a theoretical model, it is useful to determine the dependence of the observed spectral power near 418 nm upon I_L for similar hydrodynamic conditions. Using previously discussed¹⁰ analysis techniques, we determined the time at which the maximum density of the expanding plasma was $0.11n_c$ or $0.15n_c$. Figure 2 shows the dependence of the plateau level of the observed spectra power near 418 nm, under these conditions, on I_L . The data are consistent with an exponential increase but would allow saturation at the highest I_L . This increase of the spectral power near 418 nm is quite different from that of the spectral power at longer wavelengths, previously attributed to SRS.⁸ The SRS emission showed a nearly constant scattering efficiency for $I_L > 1 \times 10^{14}$ W/cm².

In order to calculate the total scattered-light signal, Eq. (1) was evaluated and the corresponding spatial gain was integrated over the plasma profile. For typical conditions, the gain region extends from $\sim 0.05\%$ to $\sim 4\%$ of n_c . The electromagnetic and electrostatic noise and the plasma opacity were properly treated, as recently discussed by Berger, Williams, and Simon,⁶ with appropriate modifications to account for the shape of the density profile and with no consideration of hot electrons. Figure 3 shows the results of these calculations under several assumptions, using a uniform laser beam of the intensity shown. The electron temperature was scaled on the basis of previous hydrodynamic simulations,¹⁰ or was taken to be $\frac{2}{3}$ of this value on the basis of previous analysis of the SRS spectrum.¹⁰ The electron density

profile was modeled as either a Gaussian or a dual exponential (symmetric about the density maximum) in space. The profile is believed to lie between these limits, which correspond to self-similar, planar, isothermal expansions from a finite or from an infinite mass source, respectively. The actual density profile at the low densities that matter here is not well known, and in similar previous experiments the measured and calculated profiles have differed at low density.¹³

The predicted gain produced by a uniform laser beam is smaller than the observed gain, which is not surprising. To evaluate the effect of the intense portions of the laser beam ("hot spots"), we included their effects using a model that has been successfully applied to previous SRS data.¹¹ The most intense hot spot was taken to have an intensity of $2.4I_L$ and a total area of 10% of the laser spot. Spatial regions on both sides of the density maximum contributed to the gain in the calculation, although in the actual plasma only some of the scattered light may pass through hot spots on both sides of the density maximum. Filamentation, which may be present, was ignored. The result of this calculation, for a dual-exponential profile with a peak density of $0.15n_c$, a scattered-light frequency of $0.82\omega_0$, and the electron temperature scaled from simulations, is shown as the solid curve in Fig. 2. One sees that this particular calculation is in rough agreement with the data. However, as Fig. 3 implies, other reasonable model assumptions could produce a calculated spectral power in conflict with the data, and most often lower than that observed. Thus, depending on the actual density profile and other factors,

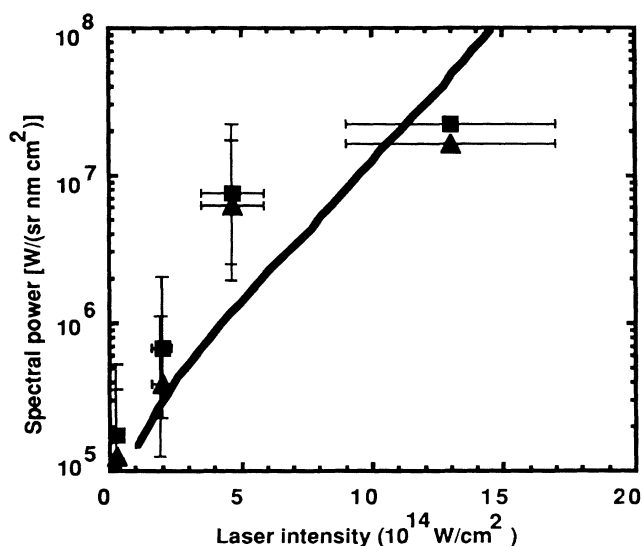


FIG. 2. The spectral power near 418 nm, from both experiment and modeling, as a function of laser intensity. The data points show the observed emission when the maximum density of the expanding plasma is $0.15n_c$ (\blacktriangle) and $0.11n_c$ (\blacksquare). The curve shows model results.

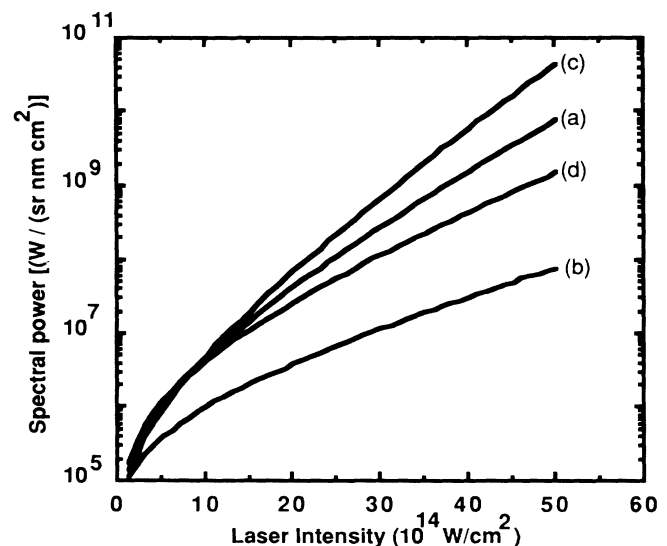


FIG. 3. The predicted spectral power of the scattered light for a uniform laser beam, under a number of assumptions. Curve *a*, the reference case, with $\omega_s = 0.82\omega_0$, T_e from simulations, and a dual-exponential density profile. Curve *b*, like *a* with a Gaussian density profile. Curve *c*, like *a* with T_e from SRS. Curve *d*, like *a* with $\omega_s = 0.86\omega_0$.

SCS-E in the initial laser beam might be completely responsible for the observed spectral power, or some intensification of the hot spots, perhaps by filamentation, might actually be present.

In conclusion, we have reported the first experimental study of SCS-E from a laser-produced plasma. Unlike thermal emission, the SCS-E increases very rapidly with laser intensity, rising more than 2 orders of magnitude from nearly thermal levels as the laser intensity increases a factor of 7 from 2×10^{14} to 1.3×10^{15} W/cm². This observation is in rough agreement with calculations that use a hot-spot model for the laser intensity distribution. In the present experiments this SCS-E emission was still much less than the SRS previously observed at lower scattered-light frequencies. However, because SCS-E depends exponentially upon an integral over the plasma profile, it will limit the ultimate size of the plasma that can be produced by a laser-fusion target. Thus, it should be evaluated as part of any thorough design of a target for laser fusion.

The authors acknowledge useful discussions with D. S. Montgomery, Dr. S. H. Batha, and Dr. B. F. Lasinski, useful discussions with and support by Dr. E. M. Campbell and Dr. J. D. Lindl, and technical support by Terry Schwinn. These experiments would not have been possible without the dedication and sustained efforts of the scientific and technical staff in all elements of the Nova Experiments Program. This work was performed under the auspices of the U.S. Department of Energy by the Lawrence Livermore National Laboratory under Contract No. W-7405-Eng-48, with partial support (T.W.J.) by the Ministère d'Éducation de Québec and the Natural Science and Engineering Research Council of Canada.

¹C. S. Liu, M. N. Rosenbluth, and R. B. White, Phys. Fluids

17, 1211 (1974).

²M. N. Rosenbluth, Phys. Rev. Lett. 29, 565 (1972).

³J. F. Drake, P. K. Kaw, Y. C. Lee, G. Schmidt, C. S. Liu, and M. N. Rosenbluth, Phys. Fluids 17, 778 (1974); D. W. Forslund, J. M. Kindel, and E. L. Lindman, Phys. Fluids 18, 1002 (1975).

⁴E. Ott, W. M. Manheimer, and H. H. Klein, Phys. Fluids 17, 1757 (1974); J. R. Albritton, Phys. Fluids 18, 51 (1975); A. T. Lin and J. M. Dawson, Phys. Fluids 18, 201 (1975).

⁵W. L. Kruer, Kent Estabrook, B. F. Lasinski, and A. B. Langdon, Phys. Fluids 23, 1326 (1980).

⁶R. L. Berger, E. A. Williams, and A. Simon, Phys. Fluids B 1, 414 (1989).

⁷D. W. Phillion, W. L. Kruer, and V. C. Rupert, Phys. Rev. Lett. 39, 1529 (1977); B. I. Cohen and A. N. Kaufman, Phys. Fluids 21, 404 (1978); A. A. Offenberger, A. Ng, and M. R. Cervenak, Can. J. Phys. 56, 381 (1978); W. L. Kruer, Phys. Fluids 23, 1273 (1980); Kent Estabrook, W. L. Kruer, and B. F. Lasinski, Phys. Rev. Lett. 45, 1399 (1980).

⁸R. P. Drake, E. A. Williams, P. E. Young, Kent Estabrook, W. L. Kruer, H. A. Baldis, and T. W. Johnston, Phys. Rev. Lett. 60, 1018 (1988).

⁹E. M. Campbell, J. T. Hunt, E. S. Bliss, D. R. Speck, and R. P. Drake, Rev. Sci. Instrum. 57, 2101 (1986).

¹⁰R. P. Drake, P. E. Young, E. A. Williams, Kent Estabrook, W. L. Kruer, B. F. Lasinski, C. B. Darrow, H. A. Baldis, and T. W. Johnston, Phys. Fluids 31, 1795 (1988).

¹¹R. P. Drake, E. A. Williams, P. E. Young, Kent Estabrook, W. L. Kruer, H. A. Baldis, and T. W. Johnston, Phys. Rev. A 39, 3536 (1989).

¹²W. Seka, E. A. Williams, R. S. Craxton, L. M. Goldman, R. W. Short, and K. Tanaka, Phys. Fluids 27, 2181 (1984); R. P. Drake, R. E. Turner, B. F. Lasinski, E. A. Williams, D. W. Phillion, Kent Estabrook, W. L. Kruer, E. M. Campbell, T. W. Johnston, K. R. Manes, and J. S. Hildum, Phys. Fluids 31, 3130 (1988).

¹³R. P. Drake, D. W. Phillion, Kent Estabrook, R. E. Turner, R. L. Kauffman, and E. M. Campbell, Phys. Fluids B 1, 1089 (1989).